Effects of a post deposition anneal on a tunneling Al2O3 interlayer for thermally stable MoOx hole selective contacts

Ah Sen, Mike Tang Soo Kiong; Melskens, Jimmy; Weeber, Arthur

DOI
10.1063/5.0097779

Publication date
2022

Document Version
Final published version

Published in
AIP Conference Proceedings

RESEARCH ARTICLE | AUGUST 24 2022

Effects of a post deposition anneal on a tunneling Al_2O_3 interlayer for thermally stable MoO_x hole selective contacts

Mike Tang Soo Kiong Ah Sen ✉; Jimmy Melskens; Arthur Weeber

AIP Conf. Proc. 2487, 020001 (2022)
https://doi.org/10.1063/5.0097779

Effects of a Post Deposition Anneal on a Tunneling Al_2O_3 Interlayer for Thermally Stable MoO_x Hole Selective Contacts

Mike Tang Soo Kiong Ah Sen[1, 2, a)], Jimmy Melskens[1], Arthur Weeber[1, 2]

[1] *TNO Solar Energy, P.O. Box 15, NL-1755 ZG Petten, The Netherlands*
[2] *Delft University of Technology, PVMD group, Mekelweg 4, NL-2628 CD Delft, The Netherlands*

[a)] Corresponding author: mike.ahsen@tno.nl

Abstract. An a-Si:H(i)/MoO_x contact gives excellent surface passivation but often leads to carrier-selectivity issues upon thermal treatments, and is limited by parasitic absorption originating from the a-Si:H(i) interlayer. Alternatively, a superior contact transparency, combined with a better hole selectivity can be obtained by replacing the a-Si:H(i) by an atomic layer deposited (ALD) Al_2O_3 interlayer. In this work, we show that good surface passivation and thermal stability at temperature up to 210 ºC, can be achieved by using this scheme. As a result, a starting efficiency of 18.2% was achieved on a 6" c-Si solar cell, with industrial processing based on screen-printing. Additionally, we showed that a post-deposition anneal (PDA) treatment on the Al_2O_3 interlayer – prior to MoO_x deposition - can further improve the surface passivation of the contact. However, such treatment also makes the contact more sensitive to ITO sputtering damage and impedes the hole transport through the Al_2O_3 interlayer.

INTRODUCTION

Passivating and carrier-selective contacts have shown to be an effective way to avoid charge carrier recombination at the metal/Si interface in homojunction c-Si solar cells. This is achieved by inserting a passivating interlayer (e.g an a-Si:H(i) or a tunneling SiO_2 interlayer) and a carrier-selective contact (e.g doped a-Si:H or poly-Si contacts) materials in between the Si absorber and metal electrodes. However, these functional layers are a source of parasitic absorption which in turn reduces the total amount of photogenerated carriers inside the Si absorber. Conversely, transparent carrier-selective contacts, such as nanocrystalline and/or alloyed Si based structures [1-3], and dopant-free metal oxides [4-6] have been explored to replace these doped Si-based contacts.

Among these dopant-free metal oxide contacts, MoO_x has shown to be a very promising hole contact with a conversion efficiency of 23.5% on a standard silicon heterojunction (SHJ) solar cell in which the p-doped a-Si:H(p) layer is replaced by MoO_x [7]. MoO_x is a wide bandgap material (~3 eV) and acts a hole selective contact material due its high work function (WF); an upward band bending is induced when contacted to Si and hence creates an asymmetric concentration of hole to electron near the Si interface, which is essential for the carrier-selectivity of the contact. However, it has been reported that the hole-carrier selectivity is lost when annealed at conditions needed to optimize SHJ solar cells [8]. The carrier selectivity loss can be partially attributed to the a-Si:H(i) interlayer which reduces the induced band bending inside the Si absorber [9], and its high valence band (E_v ~5.62 eV) which in turn impedes the transport of holes [10]. Consequently, alternative interlayers, such as Al_2O_3 have been explored to potentially replace a-Si:H(i).

Atomic Layer Deposition (ALD) of Al_2O_3 has been extensively explored for c-Si solar cells due to excellent surface passivation properties which can be explained by the excellent chemical and field effect passivation; the chemical passivation of Al_2O_3 originates from the formation of a thin SiO_2 interlayer during the initial cycles while the field effect passivation can be attributed to the high negative fixed charge density present within ~1 nm from the Si interface [11]. To achieve high level passivation, as-deposited ALD Al_2O_3 layers, typically undergo a post-deposition annealing

SiliconPV 2021, the 11th International Conference on Crystalline Silicon Photovoltaics
AIP Conf. Proc. 2487, 020001-1–020001-7; https://doi.org/10.1063/5.0097779
Published by AIP Publishing. 978-0-7354-4362-4/$30.00

(PDA) treatment that yields structural rearrangements in the Al_2O_3 bulk and interface [12, 13]. As a result, the application of Al_2O_3 as a tunneling interlayer is very attractive for the hole-selective contact. Additionally, recent studies suggest the possible implementation strategies for applying a tunneling Al_2O_3 in the solar process, and showing good recombination current density (J_0) and contact resistivity ($\rho_{contact}$) values [14, 15]. However, this concept has not yet been applied at cell level.

In this work, we investigate the possible application of an ALD Al_2O_3 interlayer in combination with an evaporated MoO_x hole-selective contact. The effect of PDA temperature (T_{PDA}) on the structural and electrical properties on the Al_2O_3 interlayer will be investigated together with its influence on the surface passivation and carrier-selectivity of the MoO_x/Al_2O_3/c-Si contact in a solar cell.

EXPERIMENTAL DETAILS

The solar cell structure explored in this paper consists of a rear ITO/poly-Si(n^+)/SiO_2 contact and a front ITO/MoO_x/Al_2O_3 contact, and is referred as the "moly-poly" solar cell of which the early potential has already been previously assessed [16]. The rear poly-Si(n^+) contact is selected due to its excellent surface passivation properties, low $\rho_{contact}$, and good thermal stability under exposure to evaluating temperature. The "moly-poly" solar cell process flow is shown in Figure 1. Note that the PDA step is performed prior to the MoO_x deposition in an N_2 environment.

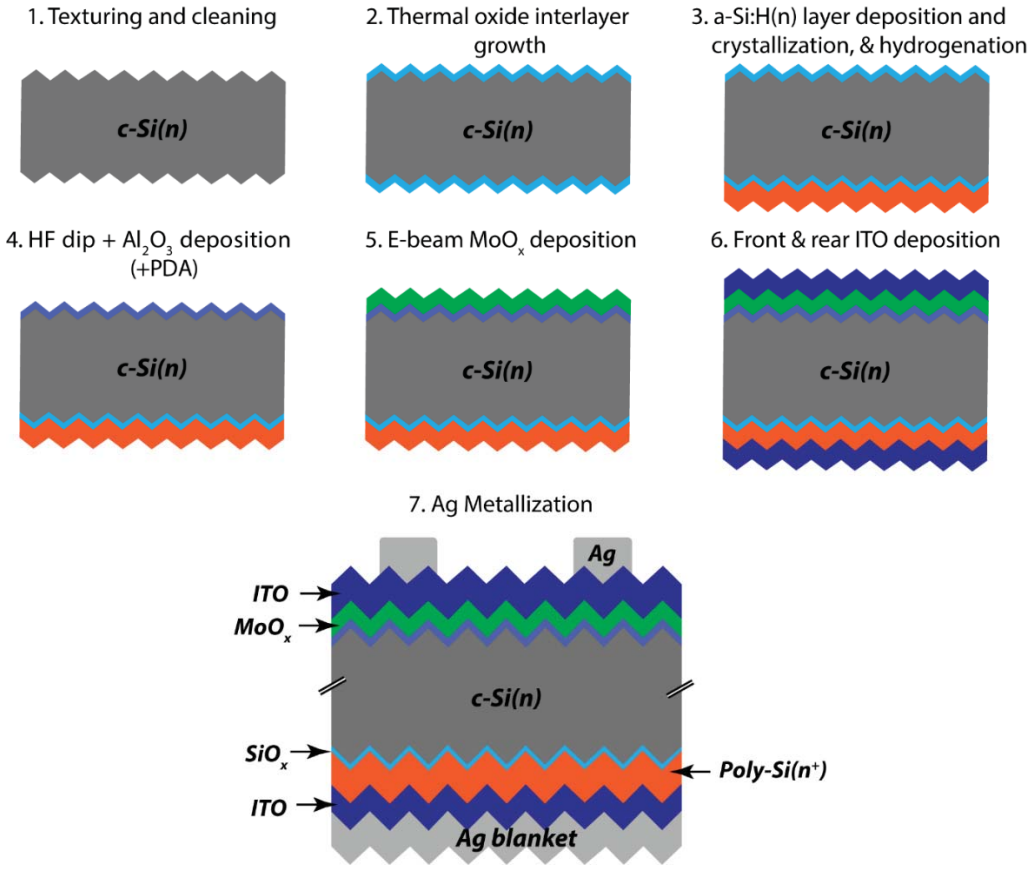

FIGURE 1. The process flow of our "moly-poly" solar cell consisting a rear poly-Si(n^+) and front MoO_x/Al_2O_3 contact. The PDA step is performed on the Al_2O_3 interlayer prior to the MoO_x deposition.

6-inch pseudo-square Cz c-Si wafers with a resistivity of ~3 Ωcm were selected, and textured in a KOH etching solution, followed by a pre-gettering step via $POCl_3$ diffusion and subsequently etched, and finished by a smoothening etch. The wafers were sequentially cleaned in an RCA 1 and 2, and NAOS solutions. Firstly, a tunneling SiO_2 layer (~1.3 nm) was thermally grown at 610 ^{0}C in a low pressure chemical vapor deposition (LPCVD) reactor. Subsequently,

a 20 nm phosphorus doped a-Si:H was deposited on the rear side of the samples by plasma enhanced chemical vapor deposition (PECVD), crystallized in an N_2 environment at 900 ^{0}C, and hydrogenated with NH_3 plasma. Next, the samples were dipped in a 1% diluted HF bath to remove the front LPCVD oxide, and subsequently the front side interlayer was deposited by 8 cycles of spatial ALD Al_2O_3 interlayer using the Levitrack from Levitech. The layers were annealed in an N_2 environment for 20 min. at temperatures ranging from 250 - 600 ^{0}C using separate samples for each T_{PDA} setting. On top of the Al_2O_3 film, a 5 nm MoO_x thin film was deposited at high vacuum ($7x10^{-6}$ mbar) in an electron beam evaporator. The deposition rate of MoO_x applied, was about 0.3 nm/s. Finally, the device was capped, on both sides, with an ITO film in a PVD sputtering tool. The rear side Ag contact was deposited by sputtering. The front Ag grid was screen printed using a low temperature Ag paste, and finally, the device was annealed in air for curing the metal print.

The injection dependent minority carrier lifetime of the samples was evaluated by transient photoconductance measurements using a Sinton WCT-120. The *IV* measurements of the solar cells were performed in a Wacom AAA solar simulator at Standard Test Conditions. The results are corrected for spectral mismatch. X-ray photoelectron spectroscopy (XPS) was performed on the oxide layers using a Thermo Scientific KA1066 spectrometer using monochromatic Al Kα X-rays source. The thickness of these AlO_x layers is determined by ellipsometry (SE, JA Woollam).

RESULTS AND DISCUSSION

Al_2O_3 Structural Properties Under PDA Treatment

Firstly, we investigated the influence of T_{PDA} (250 – 450 °C) on the film thickness and elemental composition of ALD Al_2O_3 film. Figure 2(a) shows the thickness of the deposited layers as a function of T_{PDA} determined by ellipsometry. Note that the structure formed after ALD consists of an Al_2O_3 layer and a SiO_x interfacial layer that is naturally formed during the first few ALD cycles. The as-deposited interlayer results in an average thickness of 1.43 nm and does not change upon an anneal at T_{PDA} = 250 °C. However, a significant change in layer thickness is observed at T_{PDA}=350 ^{0}C, suggesting a growth process in the overall structure during the anneal. As is shown in Figure 2(b) this growth process during the anneal can be correlated to the change in Si 2p spectra. A decrease in the Si peak is observed with increasing T_{PDA} while simultaneously Si oxidation states become more apparent which implies an increase in stoichiometry of the SiO_x layer.

Furthermore, Figure 2(c) shows that the as-deposited layer is characterized by a high O_{II}/O_I ratio which indicates the presence of residual OH groups. At this stage, no consistent Si-O and Si-H bonds are formed at the Si interface. Through a thermal treatment in an N_2 environment, the residual OH groups are dissociated to create new Si-O and Si-H bonds of which the latter passivate some of the Si dangling bonds present at the interface. However, this reaction only happens at T_{PDA}> 300 ^{0}C where the thermal energy is sufficient for the oxidation of Si by OH groups under release of H [17].

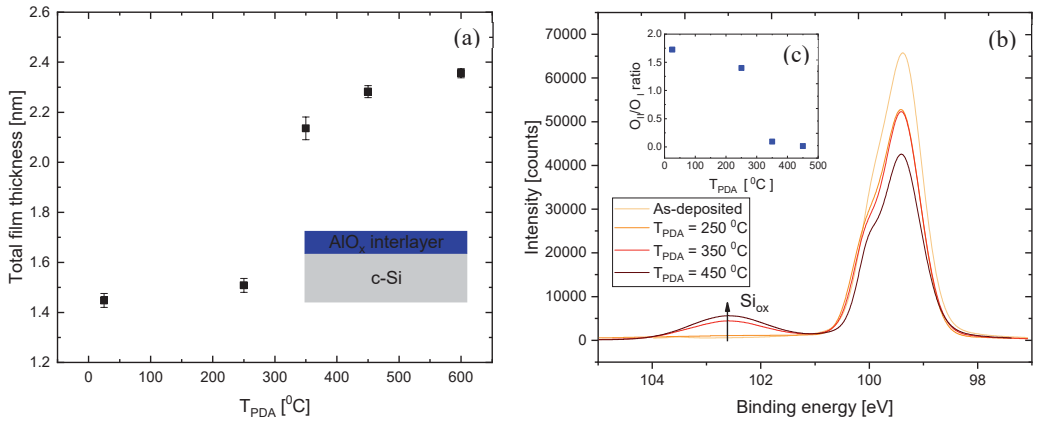

FIGURE 2. (a) Interlayer thickness as a function of T_{PDA} measured by ellipsometry, (b) XPS spectra of the Si 2p peak, (c) O_{II}/O_I ratio extracted from decomposing the O 1s spectra. Shirley background is substracted.

Surface Passivation and Contact Selectivity

In this section, we investigate the effect of T_{PDA} on the surface passivation and contact selectivity of the solar cell precursors after MoO_x and ITO films deposition (precursors are the test structures shown as steps 5 and 6, respectively, in Figure 1). Additionally, a curing anneal step is subsequently performed at SHJ conditions after ITO deposition to investigate the thermal stability of the solar cells; a curing anneal is usually performed on SHJ solar cells to ensure good contact between the metallized front grid and the ITO. The iV_{oc} of the cell precursors at each aforementioned steps is shown in the Figure 3(a). An increase in iV_{oc} after MoO_x deposition is observed with increase T_{PDA} of the ALD layer. This increase in iV_{oc} can be related to the formation of SiO_2 during this anneal as well as the possible migration of hydrogen towards the Si surface. After ITO deposition, a decrease in iV_{oc} can be noticed with increasing T_{PDA} of the ALD layer, in other words, the induced sputtering damage caused by the ITO deposition shows a dependency with the thermal budget of the PDA applied to the Al_2O_3 interlayer. It is speculated that the enhancement in Si-O coordination upon annealing is the origin of the aggravated sputtering damage on the contact. Nevertheless, further investigation is required to underpin the causes sputtering damage on the passivation quality. After performing an curing anneal at 190 °C on the precursors, the solar cell with an as-deposited Al_2O_3 interlayer shows an improvement in iV_{oc}. On the other hand, for Al_2O_3 interlayer annealed at T_{PDA} = 350 °C, the surface passivation is partially repaired after the post anneal while for the precursor with an Al_2O_3 interlayer annealed at T_{PDA} = 600 °C no significant change in iV_{oc} was noticed after the post anneal.

In terms of contact selectivity, the difference between the iV_{oc} and the external V_{oc} (ΔV) is used as figure of merit [18]. The ΔV of the solar cells with respect to T_{PDA} on the Al_2O_3 interlayer is shown in Figure 3(b); ΔV shows a dependency on the T_{PDA} carried out after ALD, where an increase in ΔV is noted with increasing T_{PDA}. After annealing, the ΔV is reduced to about 90 mV for the solar cell with an Al_2O_3 annealed at T_{PDA} = 600 °C which is still much higher compared to solar cell precursors with T_{PDA} = 350 °C or without PDA . The effect of T_{PDA} on the interlayer quality, and hence the contact selectivity, can be explained by the thickening of the interlayer which limits the tunneling transport across the interlayer. Furthermore, the formation of SiO_2 at the interface upon increasing thermal budget results in an increase in valence band offset which impedes the hole collection [19, 20]. In comparison, the MoO_x contact with an as-deposited Al_2O_3 interlayer shows excellent contact selectivity with $\Delta V < 10$ mV, both before and after the post anneal. The contact selectivity originates from an unrestricted hole transport across the interlayer.

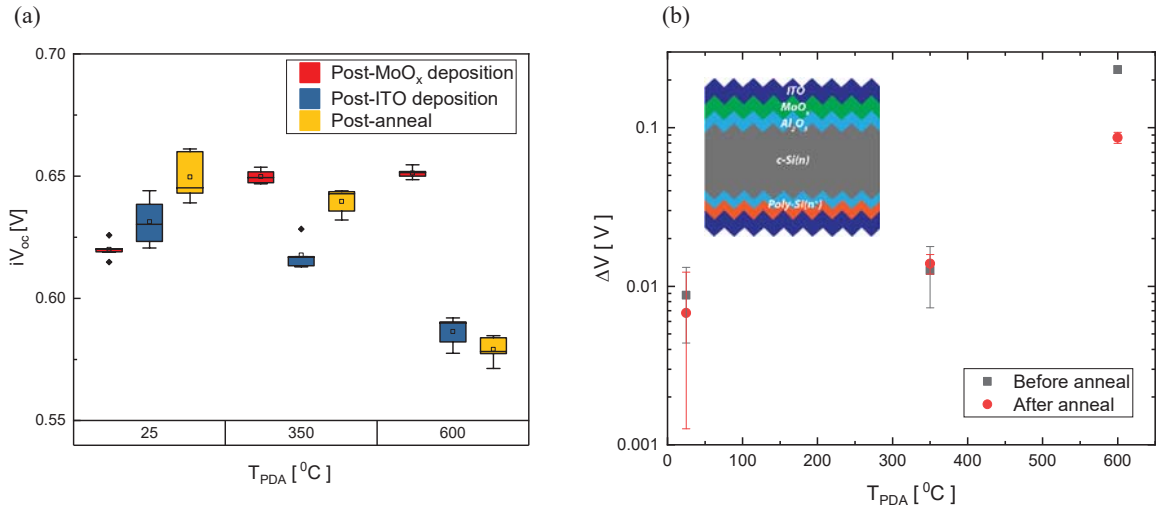

FIGURE 3. (a) iV_{oc} of the hole contact at different manufacturing stages of the hole contact at different T_{PDA}. Right: ΔV (iV_{oc} - external V_{oc}) before and after anneal (190 °C) at the specified T_{PDA}.

IV Characteristics of Completed Solar Cells

After the front metal grid was screen-printed and the rear Ag blanket was deposited, the solar cells were annealed at a curing temperature of 190 ºC for 30 min. Subsequently, the *IV* characteristics were measured and results are shown in Figure 4 and Table 1. The solar cell with an Al_2O_3 interlayer that received a PDA at T_{PDA} = 600 ºC shows a distinctive S-shaped *IV* curve with poor *FF* and V_{oc}. As expected, the effect of the S-shape *IV* curve is mitigated for solar cells with Al_2O_3 interlayer that was subjected to lower thermal budget. As a result, the best performing solar cell is obtained for the as-deposited Al_2O_3 interlayer and does not show any S-shaped IV curve characteristics. By increasing the curing anneal temperature to 210 ºC, the performance of the "moly-poly" solar cell is slightly improved, resulting in a conversion efficiency of 18.2 %. This shows that a thermally stable selectivity contact can be manufactured by using the MoO_x/Al_2O_3 contact.

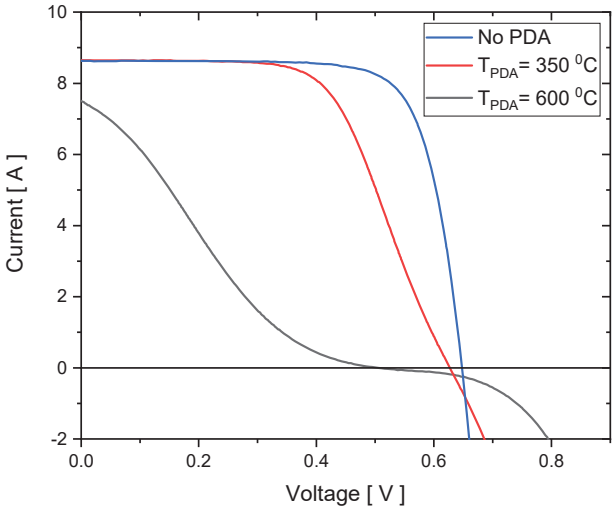

FIGURE 4. The effect of increasing T_{PDA} performed on Al_2O_3 interlayer on *IV* curve of "moly-poly" solar cells

TABLE 1. *IV* characteristics of solar cells with AlO_x interlayer treated at different temperatures

T_{PDA} of Al_2O3 interlayer [ºC]	T_{curing} [ºC]	V_{oc} [mV]	J_{sc} [mA/cm$^{2]}$	*FF* [%]	η [%]
600	190	516	32.2	20.1	3.3
350	190	628	37.2	60.3	14.1
As-deposited	190	650	36.9	75.5	18.1
As-deposited	210	651	36.9	75.6	18.2

CONCLUSIONS

In this work, we demonstrate that an ultra-thin Al_2O_3 layer, deposited by spatial ALD, can be used as an interlayer for MoO_x-based contacts in silicon solar cells. The Al_2O_3 interlayer provides surface passivation and shows excellent contact selectivity when combined with MoO_x. In addition, the thermal stability of the contact is improved without showing the presence of an S-shaped *IV* curve which is commonly observed for a MoO_x/a-Si:H(i) contact. A PDA treatment on the Al_2O_3 interlayer impedes the transport of holes - consequently causes a carrier selectivity loss, and aggravates the ITO sputtering damage. Further hydrogenation strategies and layer deposition conditions are being investigated to improve the surface passivation of the tunneling Al_2O_3 interlayer to further improve the V_{oc} of the solar cell.

ACKNOWLEDGMENTS

The authors would like to thank Bart Macco from Eindhoven University of Technology (Netherlands) for the XPS measurements, Martien Koppes, Eelko Hoek, and Benjamin Kikkert for sample fabrication, and Agnes Mewe and Gaby Janssen for the helpful discussion. This work has been financially supported by Top consortia for Knowledge and Innovation (TKI) Solar Energy programs under the "COMPASS" (TEID215022), "RADAR "(TEUE116905), and MOMENTUM (TKI Energy PPS Toeslag project number: 1821101) of the Ministry of Economic Affairs of The Netherlands.

REFERENCES

1. L. Mazzarella, S. Kirner, O. Gabriel, S.S. Schmidt, L. Korte, B. Stannowski, B. Rech, R. Schlatmann, Nanocrystalline silicon emitter optimization for Si-HJ solar cells: Substrate selectivity and CO2 plasma treatment effect, Phys. Status Solidi Appl. Mater. Sci. 214 (2017) 1532958. https://doi.org/10.1002/pssa.201532958.
2. J. Peter Seif, A. Descoeudres, M. Filipič, F. Smole, M. Topič, Z. Charles Holman, S. De Wolf, C. Ballif, Amorphous silicon oxide window layers for high-efficiency silicon heterojunction solar cells, J. Appl. Phys. 115 (2014). https://doi.org/10.1063/1.4861404.
3. A.N. Fioretti, M. Boccard, R. Monnard, C. Ballif, Low-Temperature p-Type Microcrystalline Silicon as Carrier Selective Contact for Silicon Heterojunction Solar Cells, IEEE J. Photovoltaics. 9 (2019) 1158–1165. https://doi.org/10.1109/JPHOTOV.2019.2917550.
4. C. Battaglia, S.M. De Nicolás, S. De Wolf, X. Yin, M. Zheng, C. Ballif, A. Javey, Silicon heterojunction solar cell with passivated hole selective MoO x contact, Appl. Phys. Lett. 104 (2014) 1–6. https://doi.org/10.1063/1.4868880.
5. M. Bivour, J. Temmler, F. Zahringer, S. Glunz, M. Hermle, High work function metal oxides for the hole contact of silicon solar Cells, in: 2016 IEEE 43rd Photovolt. Spec. Conf., IEEE, 2016: pp. 0215–0220. https://doi.org/10.1109/PVSC.2016.7749581.
6. L.G. Gerling, C. Voz, R. Alcubilla, J. Puigdollers, Origin of passivation in hole-selective transition metal oxides for crystalline silicon heterojunction solar cells, J. Mater. Res. 32 (2017) 260–268. https://doi.org/10.1557/jmr.2016.453.
7. J. Dréon, Q. Jeangros, J. Cattin, J. Haschke, L. Antognini, C. Ballif, M. Boccard, 23.5%-Efficient Silicon Heterojunction Silicon Solar Cell Using Molybdenum Oxide As Hole-Selective Contact, Nano Energy. 70 (2020). https://doi.org/10.1016/j.nanoen.2020.104495.
8. L. Neusel, M. Bivour, M. Hermle, Selectivity issues of MoOxbased hole contacts, Energy Procedia. 124 (2017) 425–434. https://doi.org/10.1016/j.egypro.2017.09.268.
9. S. Essig, J. Dréon, E. Rucavado, M. Mews, T. Koida, M. Boccard, J. Werner, J. Geissbühler, P. Löper, M. Morales-Masis, L. Korte, S. De Wolf, C. Balllif, Toward Annealing-Stable Molybdenum-Oxide-Based Hole-Selective Contacts For Silicon Photovoltaics, Sol. RRL. 1700227 (2018) 1700227. https://doi.org/10.1002/solr.201700227.
10. C. Messmer, M. Bivour, J. Schön, S.W. Glunz, M. Hermle, J. Schon, S.W. Glunz, M. Hermle, Numerical Simulation of Silicon Heterojunction Solar Cells Featuring Metal Oxides as Carrier-Selective Contacts, IEEE J. Photovoltaics. 8 (2018) 456–464. https://doi.org/10.1109/JPHOTOV.2018.2793762.
11. G. Dingemans, W.M.M. Kessels, Status and prospects of Al_2O_3 -based surface passivation schemes for silicon solar cells, J. Vac. Sci. Technol. A Vacuum, Surfaces, Film. 30 (2012) 040802. https://doi.org/10.1116/1.4728205.
12. B. Hoex, J. Schmidt, P. Pohl, M.C.M. van de Sanden, W.M.M. Kessels, Silicon surface passivation by atomic layer deposited Al2O3, J. Appl. Phys. 104 (2008) 044903. https://doi.org/10.1063/1.2963707.
13. G. Dingemans, P. Engelhart, R. Seguin, F. Einsele, B. Hoex, M.C.M. Van De Sanden, W.M.M. Kessels, Stability of Al2O3 and Al2O3/a- SiNx:H stacks for surface passivation of crystalline silicon, J. Appl. Phys. 106 (2009). https://doi.org/10.1063/1.3264572.
14. Z. Xin, Z.P. Ling, P. Wang, J. Ge, C. Ke, K.B. Choi, A.G. Aberle, R. Stangl, Ultra-thin atomic layer deposited aluminium oxide tunnel layer passivated hole-selective contacts for silicon solar cells, Sol. Energy Mater. Sol. Cells. (2019). https://doi.org/10.1016/j.solmat.2018.11.011.

15. G. Gregory, C. Feit, Z. Gao, P. Banerjee, T. Jurca, K.O. Davis, Improving the Passivation of Molybdenum Oxide Hole-Selective Contacts with 1 nm Hydrogenated Aluminum Oxide Films for Silicon Solar Cells, Phys. Status Solidi Appl. Mater. Sci. 217 (2020) 1–7. https://doi.org/10.1002/pssa.202000093.
16. P. Spinelli, M.A. Sen, E.G. Hoek, B.W.J. Kikkert, G. Yang, O. Isabella, A.W. Weeber, P.C.P. Bronsveld, Moly-poly solar cell: Industrial application of metal-oxide passivating contacts with a starting efficiency of 18.1%, in: AIP Conf. Proc., American Institute of Physics Inc., 2018: p. 040021. https://doi.org/10.1063/1.5049284.
17. G. Dingemans, W. Beyer, M.C.M. Van De Sanden, W.M.M. Kessels, Hydrogen induced passivation of Si interfaces by Al2 O 3 films and SiO2/Al2 O3 stacks, Appl. Phys. Lett. 97 (2010) 2008–2011. https://doi.org/10.1063/1.3497014.
18. L.G. Gosset, J.F. Damlencourt, O. Renault, D. Rouchon, P. Holliger, A. Ermolieff, I. Trimaille, J.J. Ganem, F. Martin, M.N. Séméria, Interface and material characterization of thin Al2O3 layers deposited by ALD using TMA/H2O, J. Non. Cryst. Solids. 303 (2002) 17–23. https://doi.org/10.1016/S0022-3093(02)00958-4.
19. Bivour, M., Messmer, C., Neusel, L., Zähringer, F., Schön, J., Glunz, S., & Hermle, M. (2017, September). Principles of carrier-selective contacts based on induced junctions. In 33rd European PV Solar Energy Conference and Exhibition, Amsterdam, The Netherlands (pp. 25-29).17.
20. M. Liebhaber, M. Mews, T.F. Schulze, L. Korte, B. Rech, K. Lips, Valence band offset in heterojunctions between crystalline silicon and amorphous silicon (sub)oxides (a-SiOx:H, 0 < x < 2), Appl. Phys. Lett. 106 (2015) 0–5. https://doi.org/10.1063/1.4906195.
21. J.P. Seif, D. Menda, A. Descoeudres, L. Barraud, O. Özdemir, C. Ballif, S. De Wolf, Asymmetric band offsets in silicon heterojunction solar cells: Impact on device performance, J. Appl. Phys. 120 (2016). https://doi.org/10.1063/1.4959988.